Quasiparticle energy bands of NiO in the *GW* approximation

Je-Luen Li, G.-M. Rignanese,* and Steven G. Louie
Department of Physics, University of California at Berkeley, Berkeley, California 94720
and Materials Sciences Division, Lawrence Berkeley National Laboratory, Berkeley, California 94720, USA
(Received 10 March 2005; published 26 May 2005)

We present a first-principles study of the quasiparticle excitations spectrum of NiO. The calculations are performed using the spin-polarized *GW* approximation in a plane-wave basis set with *ab initio* pseudopotentials. We find a feature in the band structure which can explain both an absorption edge of 3.1 eV in optical measurements and an energy gap of 4.3 eV found in XPS/BIS measurements. The calculated quasiparticle density of states shows that the oxygen 2*p* peaks overlap with the satellite structure at ~8 eV below the Fermi level. Finally, we discuss the difference between this work and two previous quasiparticle energy calculations.

DOI: 10.1103/PhysRevB.71.193102 PACS number(s): 71.20.Ps, 71.15.Qe, 71.45.Gm

Since the early days of band theory, NiO has been one of the most intensively studied transition metal mono-oxides. In a purely ionic picture of NiO, the Ni ions have a partially filled 3*d* shell which should result in a metallic behavior according to conventional band theory. However, experimentally, NiO is found to be an insulator. The value of ~4 eV is most often cited for the fundamental gap,[1,2] but this value needs to be taken with caution. Indeed, the measured optical absorption coefficient of NiO shows an onset of absorption at 3.1 eV and reaches its maximum at 4.3 eV.[3] Very similar results are also obtained from UV-isochromat on oxidized nickel[4] and electron energy-loss spectroscopy.[5]

Understanding the electronic structure of NiO is a topic of great interest both for experimentalists and theorists, which has given rise to some controversy in the literature. For a long time, NiO was considered as a prototype Mott insulator in which the insulating gap is caused by the on-site Coulomb energy U.[6] However, this view was challenged based on photoemission and inverse photoemission measurements and model calculations.[1,2] It was proposed that NiO should be categorized as a charge-transfer insulator, the gap resulting predominantly from a $d^8+d^8 \rightarrow d^8L+d^9$ intercluster transition (L denotes a ligand 2*p* hole). This latter explanation has gained a wide acceptance since it is able to explain most of the experimental data. However, Hüfner *et al.*[7] recently reinvestigated the experiment and concluded that it could not be excluded that the optical gap in pure NiO corresponds to the transition from Ni 3*d* bands into an empty 3*d* band.

Standard band-structure calculations in the local spin density approximation[8] (LSDA) produce a gap (0.3 eV) which is one order of magnitude smaller than the measured band gap. The calculated magnetic moment is also much smaller than the experimental data. These are the key reasons to question the validity of mean field one-electron band theory to describe the electronic structure of NiO. There have been several attempts to calculate the NiO band structure beyond the LSDA. For localized states (e.g., 3*d* electron states), the generalized gradient approximation (GGA) allows one to take into account more the effects of varying density than the LSDA. Some recent publications[9–12] using Kohn-Sham energy eigenvalues from the GGA, however, gave quite a wide range of band gaps (from 0.5 to 1.2 eV) for NiO. The discrepancy may come from that the angular gradient is not properly taken into account in some studies and thus a smaller band gap.[10] Other "improved" computational schemes such as the self-interaction corrected density functional theory (DFT) and the model LSDA+U methods have also been applied to transition metal oxides.[13–15] Beyond the methods based on DFT, a Green's function approach using the *GW* approximation has been shown to be quite accurate in calculating the quasiparticle excitations for a wide variety of semiconductors and insulators.[16,17] Lately, a few quasiparticle band structure calculations have also been conducted for NiO.[18–20] However, despite all these studies rely on LSDA calculations as a starting guess for constructing the electron self-energy operator, the energy gaps obtained do not agree with each other. This is due to the underlying different approximations, self-consistency, and assumptions used.

Recently, we have demonstrated in the framework of the study of the metal-insulator transition in solid hydrogen that the band gaps calculated by LSDA+*GW* and GGA+*GW* methods differ.[21] Moreover, it was found that the GGA +*GW* method is in better agreement with VQMC and experiment. The difference was attributed to the LSDA and GGA energy spectrum, the GGA eigenfunctions and eigenvalues being closer to the quasiparticle calculation results. In particular, for localized 3*d* electron states, GGA takes into account the moderately varying density rather than LSDA which is based on results of the homogeneous electron gas. Hence, using the GGA as a starting point for the *GW* method seems the obvious next step towards the understanding of the NiO electronic structure. This is the aim of the present study.

In this Brief Report, we present *ab initio* quasiparticle (QP) calculations of NiO in the *GW* approximation. The quasiparticle band structure is compared to the detailed angle-resolved photoemission spectra (ARPES) data. With this quasiparticle band structure, it is possible to explain both the optical absorption edge seen in optical measurements and the fundamental gap found in photoemission (XPS) and inverse photoemission (BIS) experiments. The quasiparticle density of states (DOS) is obtained using the quasiparticle energies and is in good agreement with experiment. Finally, we discuss the difference between this work and previous quasiparticle energy calculations.

Below the Néel temperature, NiO has a type-II antiferromagnetic ordering and (nearly) cubic structure. In our calculation, we assume an ideal rocksalt structure with lattice constant 4.1767 Å. The spins of Ni atoms are ferromagnetically aligned within the {111} planes, but are in antiferromagnetic array along the [111] direction.

In our GGA calculations, only valence electrons are explicitly considered using pseudopotentials to account for core-valence interactions. However, for the quasiparticle bandstructure calculations, it has been shown[22] that the shallow core shells need to be included as valence states when there is significant overlap between core and valence electron orbitals. Thus the Ni 3*s* and 3*p* orbitals are treated here as valence states in the pseudopotential. The cutoff radii of the Ni *s*, *p* and *d* pseudopotentials are set at 0.8 a.u. The wave functions are expanded on a plane-wave basis set. Due to the inclusion of Ni 3*s* and 3*p* states as valence electrons, an energy cutoff of 200 Ry is used to ensure a good convergence of the calculated properties. Summations over the Brillouin zone were carried out using an $8\times8\times4$ Monkhorst-Pack[23] grid. The exchange and correlation energy is evaluated using the Perdew-Burke-Ernzerhof[24] parametrization.

The details of our spin-polarized *GW* scheme can be found in a recently published paper.[21] We compute the static dielectric matrix $\epsilon^{-1}_{\mathbf{G},\mathbf{G}'}(\mathbf{q},\omega=0)$ in the random phase approximation (RPA) only for **G** vectors of kinetic energy smaller than 58 Ry. The dielectric matrix at finite frequencies is obtained using a generalized plasmon-pole model.[17] The self-energy Σ is obtained by summing over eight special *q* points in the irreducible Brillouin zone, and over 84 bands (24 occupied and 60 unoccupied bands). The self-energy calculation is performed by updating the new quasiparticle energies obtained from one iteration to construct the Green's function for the next iteration. We start from $\Psi_{\mathrm{QP}}=\Psi_{\mathrm{GGA}}$ and use second order perturbation to compute energy correction terms to the quasiparticle energies. As we did not find any large off-diagonal element for the operator $\Sigma-V_{\mathrm{xc}}$, we assume for all the iterations that $\Psi_{\mathrm{QP}}\approx\Psi_{\mathrm{GGA}}$.

To compute the density of states with sufficiently dense **k**-point sampling, we used an interpolation scheme[25] to approximate quasiparticle energies at nearby **k** points. The self-energy operator matrix element at a fine grid $\{\mathbf{k}\}$ can be approximated by a set of matrix elements at a nearby coarse-grid $\tilde{\mathbf{k}}$ point (*m* denotes band indices):

$$\langle n\mathbf{k}|\Sigma|n\mathbf{k}\rangle=\sum_{m,m'} d^{n\mathbf{k}}_{m\tilde{\mathbf{k}}}d^{m'\tilde{\mathbf{k}}}_{n\mathbf{k}}\langle m\tilde{\mathbf{k}}|\Sigma|m'\tilde{\mathbf{k}}\rangle, \tag{1}$$

where $d^{n\mathbf{k}}_{m\tilde{\mathbf{k}}}=\int d\mathbf{r}\,\psi^*_{n\mathbf{k}}(\mathbf{r})e^{i(\mathbf{k}-\tilde{\mathbf{k}})}\psi_{m\tilde{\mathbf{k}}}(\mathbf{r})$. In most cases $\langle m\tilde{\mathbf{k}}|\Sigma-V_{\mathrm{xc}}|m'\tilde{\mathbf{k}}\rangle$ is almost diagonal. Thus we have

$$\langle n\mathbf{k}|\Sigma-V_{\mathrm{xc}}|n\mathbf{k}\rangle\approx\sum_m |d^{n\mathbf{k}}_{m\tilde{\mathbf{k}}}|^2\langle m\tilde{\mathbf{k}}|\Sigma-V_{\mathrm{xc}}|m\tilde{\mathbf{k}}\rangle. \tag{2}$$

The error involved in the interpolation when extending data from 32 **k** points to 128 **k** points is less than 0.2 eV.

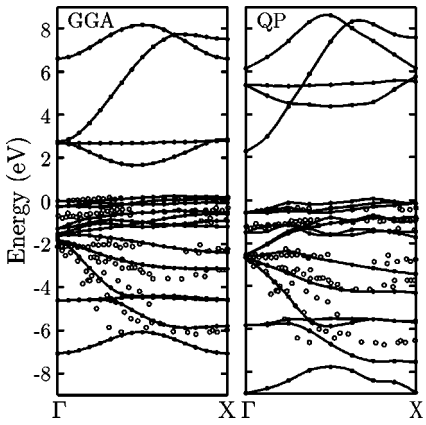

FIG. 1. GGA and quasiparticle (QP) band structures of NiO along the Γ*X* line. The open circles are taken from ARPES data (Ref. 26).

The calculated GGA and quasiparticle band structures are shown in Fig. 1. The most obvious difference between the *GW* and GGA results is the upward shift of unoccupied *d* bands by 2.5 eV (the top of valence band is aligned at 0 eV). This opens the quasiparticle energy gap between occupied and unoccupied *d* bands to 4.2 eV. Another important result is that near the Γ point, the position of the unoccupied *s*-like band changes little relative to the occupied *d* states, and produces a 2.9 eV *d*-*s* energy gap at Γ. This is an interesting new feature found in the NiO quasiparticle band structure. Since the phase space of the low-lying unoccupied *s*-like states is very small in the Brillouin zone, our results can account for both the beginning of the strong optical absorption at 3.1 eV and the first peak at 4.3 eV. A comparison of the calculated density of states with XPS/BIS measurement is shown in Fig. 2. The peak-to-peak separation in the calculated DOS matches the experimental data very well.

In the band structures of Fig. 1, note that there are no available states at 8 eV below the Fermi level in the GGA band structure, while in the *GW* calculation the occupied oxygen bands are pushed down to this energy range where strong satellite structures are observed experimentally. This is in accord with resonance photoemission experiments[27] which suggest an inseparable overlap between O 2*p* states and the satellite structure.

In Fig. 1, we also compare the calculated GGA and quasiparticle band structures to ARPES data[26] along the [100]

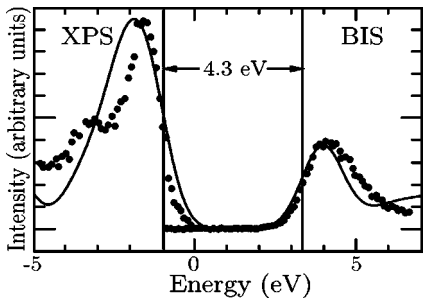

FIG. 2. Comparison between XPS/BIS measurements (dots) (Ref. 1) and calculated quasiparticle density of states. A Gaussian broadening of 0.6 eV, which is the resolution of the experiment in Ref. 1, is used.

direction. Along the ΓX direction, the oxygen states belong to the C_{4v} symmetry group if we assume a perfect rocksalt structure; thus the oxygen Δ_1 and Δ_5 bands are degenerate at the Γ point. This is used to align our calculations with the energy position of the experimental data in Fig. 1. The LSDA bands[26] agree well with most of ARPES data, in particular the oxygen bands dispersion. However, the energy separation between the Ni 3*d* and O 2*p* bands is not correct, and the dispersion of Ni 3*d* band which lies above the O 2*p* states is too large. The GGA band structure gives smaller Ni 3*d* bandwidth, but the absence of the theoretical bands just below the Fermi level (at ~ -1 eV) is an obvious departure from the ARPES data. In the quasiparticle energy band structure, we find a good agreement for the relative positions of the O 2*p* bands and Ni 3*d* bands at the Γ point. The theoretical *GW* Ni 3*d* bands are at the correct energy positions, and the separation between different bands fit well with observed data. In particular, the energy location and the dispersion of the bands in the range -2 to -3 eV are in better agreement with ARPES data than either GGA or LSDA bands. We note in the experiment, the oxygen derived bands show very strong emission angle dependence which makes it more difficult to compare with the calculations. With this in mind, the *GW* calculation does seem to improve the agreement between theory and experiment.

The detailed characters of the valence bands has also been a subject of debate. In the original Mott insulator picture, the Ni 3*d* band is split by the on-site Coulomb interaction into upper and lower Hubbard bands with the lower Hubbard band completely filled. A current picture, perhaps more widely accepted, however, adopts a cluster model explanation in which the hybridization between the O 2*p* and the Ni 3*d* states pushes up the strongly hybridized oxygen states to the top of the valence band. In our calculations, we have assumed that $\Psi_{\mathrm{QP}} \approx \Psi_{\mathrm{GGA}}$ since we did not find any large off-diagonal element of the operator $\Sigma - V_{\mathrm{xc}}$ between the GGA Ni 3*d* states and O 2*p* states, although there is some mixing between unoccupied and occupied Ni 3*d* bands. Our analysis therefore relies on GGA results. We project the GGA wave functions to angle-resolved components centered at each atom, taking atomic sphere radii for Ni and O of 2.1 and 1.8 a.u., respectively. We find that in fact the 3*d* bands contain significant O 2*p* components. The occupied 3*d* wave functions at Γ have approximately 20% weight of O 2*p* states. Conversely, the O 2*p* bands contain significant Ni 3*d* weight ranging from 11 to 41 %. The appearance of the mainly *d* character satellite at ~ -8 eV should further "remove *d* spectral weight" from the valence states near the Fermi level.[18]

Our results differ considerably from two previous quasiparticle calculations[18,19] where the 4*s* band was found to lay above the lowest unoccupied 3*d* band. The band gap at the Γ point was at least 5.5 eV in Ref. 18 and $\sim$5.5 eV in Ref. 19. The unique feature that we obtain originates from the shifting of the 4*s* band under the *GW* approximation. Indeed, in our calculations, the *GW* correction of the energies of (delocalized) 4*s* states is much less than those of (more localized) *d* states, whereas in the previous studies the 4*s* band seems to be shifted by roughly the same amount as the unoccupied 3*d* bands (i.e., $\sim$2.5 eV upwards). As a result, our band gap at Γ is between the occupied 3*d* bands and the 4*s* band, whereas it is between the occupied and unoccupied 3*d* bands in the previous studies. If we now consider the band gap between occupied and unoccupied *d* states, our result of 4.2 eV falls right in between the two reported values. In fact, our results show a better agreement with the more recent work of Faleev *et al.*[20] In particular, they also found the conduction-band minimum falls at the Γ point. However, their overall band gap (4.8 eV) is larger than ours.

The origin of these discrepancies calls for a more detailed discussion. The main difference in the methods of this work with respect to the previous ones resides in the starting point of the *GW* approximation. Our zeroth order term is constructed from the result of a GGA calculation, whereas the previous studies adopt the result of a LSDA calculation. This has important consequences.

In the work of Aryasetiawan and Gunnarsson,[18] the dielectric function is calculated within the LSDA-RPA. For comparison purposes, we also compute the dielectric matrix using LSDA eigenfunctions and eigenvalues. Due to the nearly zero band gap in the LSDA, we obtain a dielectric constant $\epsilon_0 = 35.8$, which is much larger than the measured value of 5.4–5.8.[3,28] When we work within the GGA-RPA, we find $\epsilon_0 = 13.1$ which is much better though still larger than the experimental data. The GGA also gives significant improvement of the magnetic moment ($1.6\mu_B$) over the LSDA [$1.12\mu_B$ (Ref. 8)]. [The measured magnetic moment is 1.6–$1.9\mu_B$ (Refs. 29–31).] This is a clear divergence between these two studies. Another important difference is related to the manner in which the self-consistency in the Green's function is achieved. After performing *GW* calculations with unmodified GGA wave functions and eigenvalues, we reenter the resulting QP energies into the Green's functions without updating wave functions ($\Psi_{\mathrm{QP}} \approx \Psi_{\mathrm{GGA}}$). In Ref. 18, the self-consistency requirement in the gap is simulated by applying a nonlocal potential to the e_g orbital. The effect of this approximation still remains to be checked.

In the work of Massida *et al.*,[19] the difficulties related to the dielectric matrix are circumvented by approximating the dielectric response with a simple model. It should, however, be emphasized that by using two different models the band gaps were found to differ by as much as 0.4 eV. Also, instead of calculating the energy-dependent Green's function, a density matrix is used in this model *GW* scheme. We find that energy-dependent Green's function plays an important role in this system. Moreover, our calculation shows a better agreement with ARPES data especially at the higher binding energy region, where noticeable deviation can be seen in model *GW* band structures (Fig. 3 of Ref. 19).

Finally, we briefly remark that the constrained self-consistent *GW* method by Faleev *et al.*[20] contains several new additions in the theory (all-electron, full-potential, self-consistency in both wave functions and energies). This *GW* scheme should be independent of the starting approximation. It is thus reassuring that when we employ a better starting guess (GGA), the calculated energy bands share several similarities with those of Ref. 20, in particular the location of the conduction-band minimum.

In brief, we performed spin-polarized *GW* calculations for NiO using a plane-wave basis. Within this formalism, we have calculated the quasiparticle band structure and found interesting features. The agreement between calculated and experimental (ARPES) band structure is improved compared with LDA or GGA results. In addition to a 4.2 eV band gap which separates the empty *d* states from the valence bands, new features found in the quasiparticle band structure include a lowest *s*-like conduction band at the Γ point which forms an energy gap of 2.9 eV. This picture is consistent with the observed onset of optical absorption at 3.1 eV and a fundamental band gap at 4.3 eV found in BIS-XPS. We also found oxygen 2*p* states at ~8 eV below the Fermi level where satellite structures are observed.

ACKNOWLEDGMENTS

This work was supported by the National Science Foundation Grant No. DMR00-87088, and by the Director, Office of Science, Office of Basic Energy Sciences, Materials Sciences Division of the U.S. Department of Energy under Contract No. DE-AC03-76SF00098. Computational resources have been provided by the DOE at the National Energy Research Scientific Computing Center.

*Present address: Université Catholique de Louvain, Unité de Physico-Chimie et de Physique des Matériaux, Place Croix du Sud, 1, B-1348 Louvain-la-Neuve, Belgium

[1] G. A. Sawatzky and J. W. Allen, Phys. Rev. Lett. **53**, 2339 (1984).
[2] S. Hüfner, J. Osterwalder, T. Riesterer, and F. Hulliger, Solid State Commun. **52**, 793 (1984).
[3] R. J. Powell and W. E. Spicer, Phys. Rev. B **2**, 2182 (1970).
[4] H. Scheidt, M. Glöbl, and V. Dose, Surf. Sci. **112**, 97 (1981).
[5] A. Gorschlüter and H. Merz, Int. J. Mod. Phys. B **7**, 341 (1993).
[6] B. H. Brandow, Adv. Phys. **26**, 651 (1977).
[7] S. Hüfner, P. Steiner, I. Sander, F. Reinert, and H. Schmitt, Z. Phys. B: Condens. Matter **86**, 207 (1992).
[8] K. Terakura, T. Oguchi, A. R. Williams, and J. Kübler, Phys. Rev. B **30**, 4734 (1984).
[9] T. C. Leung, C. T. Chan, and B. N. Harmon, Phys. Rev. B **44**, 2923 (1991).
[10] P. Dufek, P. Blaha, V. Sliwko, and K. Schwarz, Phys. Rev. B **49**, 10 170 (1994).
[11] S. L. Dudarev, L.-M. Peng, S. Y. Savrasov, and J.-M. Zuo, Phys. Rev. B **61**, 2506 (2000).
[12] T. Bredow and A. R. Gerson, Phys. Rev. B **61**, 5194 (2000).
[13] A. Svane and O. Gunnarsson, Solid State Commun. **76**, 851 (1990).
[14] Z. Szotek, W. M. Temmerman, and H. Winter, Phys. Rev. B **47**, 4029 (1993).
[15] V. I. Anisimov, J. Zaanen, and O. K. Andersen, Phys. Rev. B **44**, 943 (1991).
[16] L. Hedin, Phys. Rev. **139**, A796 (1965).
[17] M. S. Hybertsen and S. G. Louie, Phys. Rev. B **34**, 5390 (1986).
[18] F. Aryasetiawan and O. Gunnarsson, Phys. Rev. Lett. **74**, 3221 (1995).
[19] S. Massidda, A. Continenza, M. Posternak, and A. Baldereschi, Phys. Rev. B **55**, 13 494 (1997).
[20] S. V. Faleev, M. van Schilfgaarde, and T. Kotani, Phys. Rev. Lett. **93**, 126406 (2004).
[21] J.-L. Li, G.-M. Rignanese, E. K. Chang, X. Blase, and S. G. Louie, Phys. Rev. B **66**, 035102 (2002).
[22] M. Rohlfing, P. Krüger, and J. Pollmann, Phys. Rev. Lett. **75**, 3489 (1995).
[23] H. J. Monkhorst and J. D. Pack, Phys. Rev. B **13**, 5188 (1976).
[24] J. P. Perdew, K. Burke, and M. Ernzerhof, Phys. Rev. Lett. **77**, 3865 (1996).
[25] M. Rohlfing and S. G. Louie, Phys. Rev. Lett. **81**, 2312 (1998).
[26] Z.-X. Shen *et al.*, Phys. Rev. B **44**, 3604 (1991).
[27] S. J. Oh, J. W. Allen, I. Lindau, and J. C. Mikkelsen, Phys. Rev. B **26**, 4845 (1982).
[28] K. V. Rao and A. Smakula, J. Appl. Phys. **36**, 2031 (1965).
[29] B. E. F. Fender, A. J. Jacobson, and F. A. Wegwood, J. Chem. Phys. **48**, 990 (1968).
[30] H. A. Alperin, J. Phys. Soc. Jpn. **17**, 12 (1962).
[31] A. K. Cheetham and D. A. O. Hope, Phys. Rev. B **27**, 6964 (1983).